

Supporting Information

g-C₃N₄ Promoted MOF Derived Hollow Carbon Nanopolyhedra Doped with High Density/Fraction of Single Fe Atoms as an Ultra-High Performance Non-precious Catalyst towards Acidic ORR and PEM Fuel Cell

*Yijie Deng^{a§b}, Bin Chi^{a§}, Xinlong Tian^a, Zhiming Cui^a, Ershuai Liu^d, Qingying Jia^d,
Wenjun Fan^a, Guanghua Wang^a, Dai Dang^a, Minsi Li^c, Ketao Zang^e, Jun Luo^e,
Yongfeng Hu^f, Shijun Liao^{a*}, Xueliang Sun^{c*}, Sanjeev Mukerjee^d*

^aThe Key Laboratory of Fuel Cell Technology of Guangdong Province, School of Chemistry and Chemical Engineering, South China University of Technology, Guangzhou 510641, China

^bSchool of Environment and Civil Engineering, Dongguan University of Technology, Dongguan, China

^cDepartment of Mechanical and Materials Engineering, University of Western Ontario, 1151 Richmond St., London, Ontario, Canada N6A 3K7

^dDepartment of Chemistry and Chemical Biology, Northeastern University, Boston, Massachusetts, 02115, USA.

^eCenter for Electron Microscopy, TUT-FEI Joint Laboratory, Tianjin Key Laboratory of Advanced Functional Porous Materials, Institute for New Energy Materials & Low-Carbon Technologies, School of Materials Science

and Engineering, Tianjin University of Technology, Tianjin 300384 (China)

^fCanadian Light Source 44 Innovation Boulevard Saskatoon, SK, Canada S7N 2V3

* Corresponding authors, chsjliao@scut.edu.cn, xsun9@uwo.ca

§Deng and Chi contributed equally to this work.

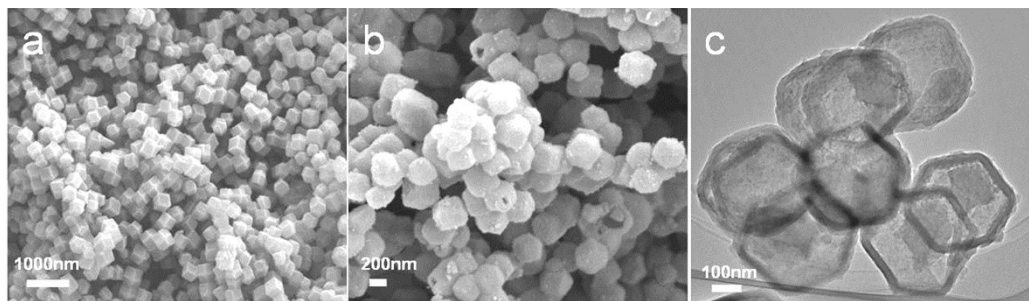


Fig. S1 SEM of the pristine ZIF-8(a) and hollow ZIF-8(b), and TEM of hollow ZIF-8(c)

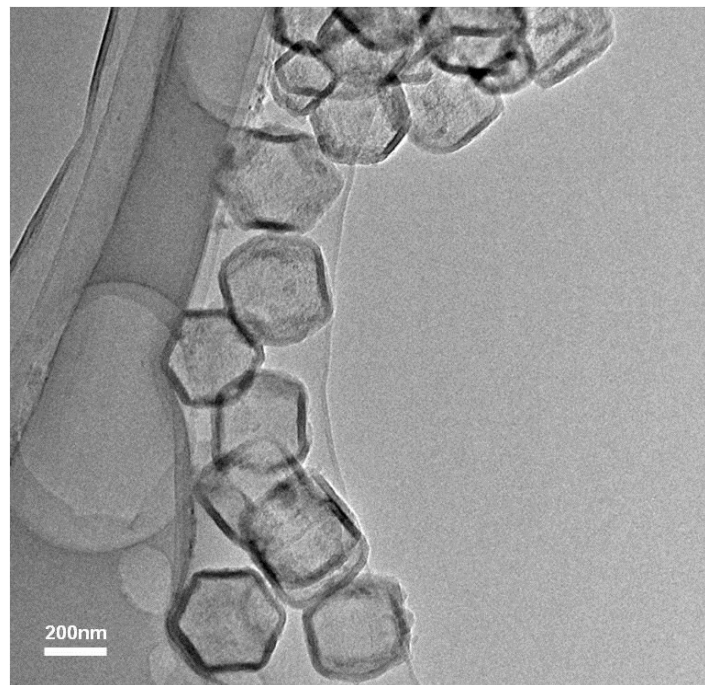


Fig. S2 TEM of sample C-FeHZ8@g-C₃N₄-950 with large scale range

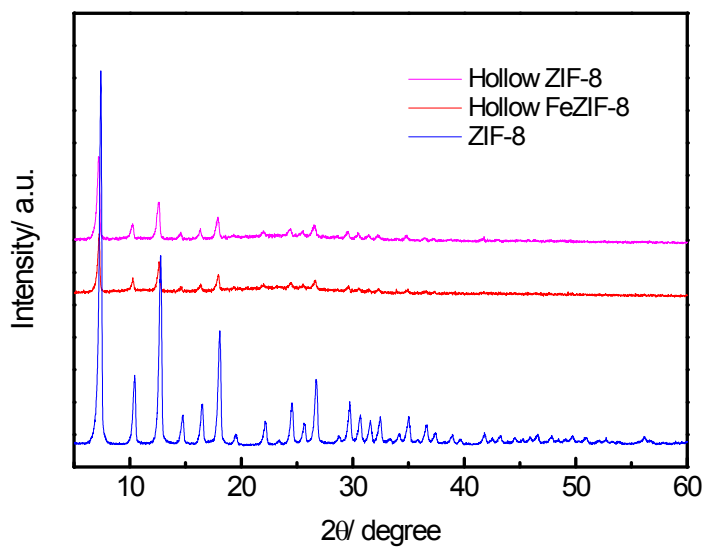


Fig. S3 PXRD of the ZIF-8, hollow ZIF-8, and hollow FeZIF-8

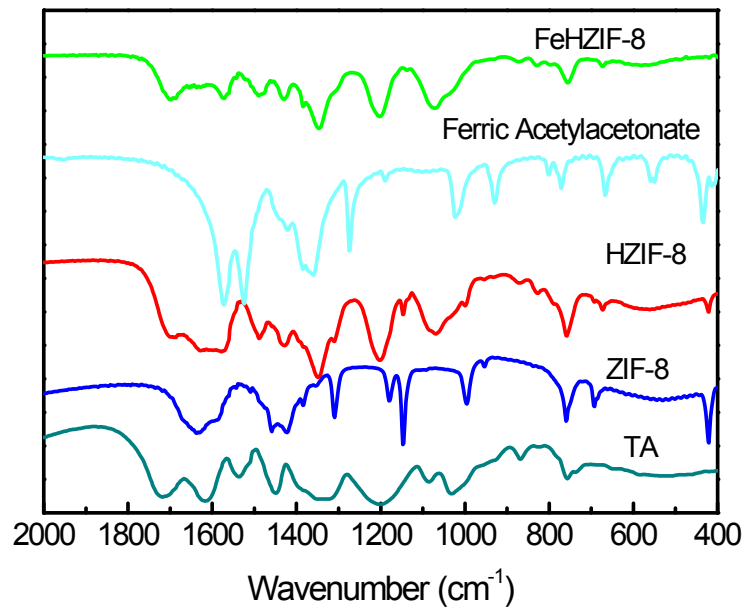


Fig. S4 FTIR spectra of materials.

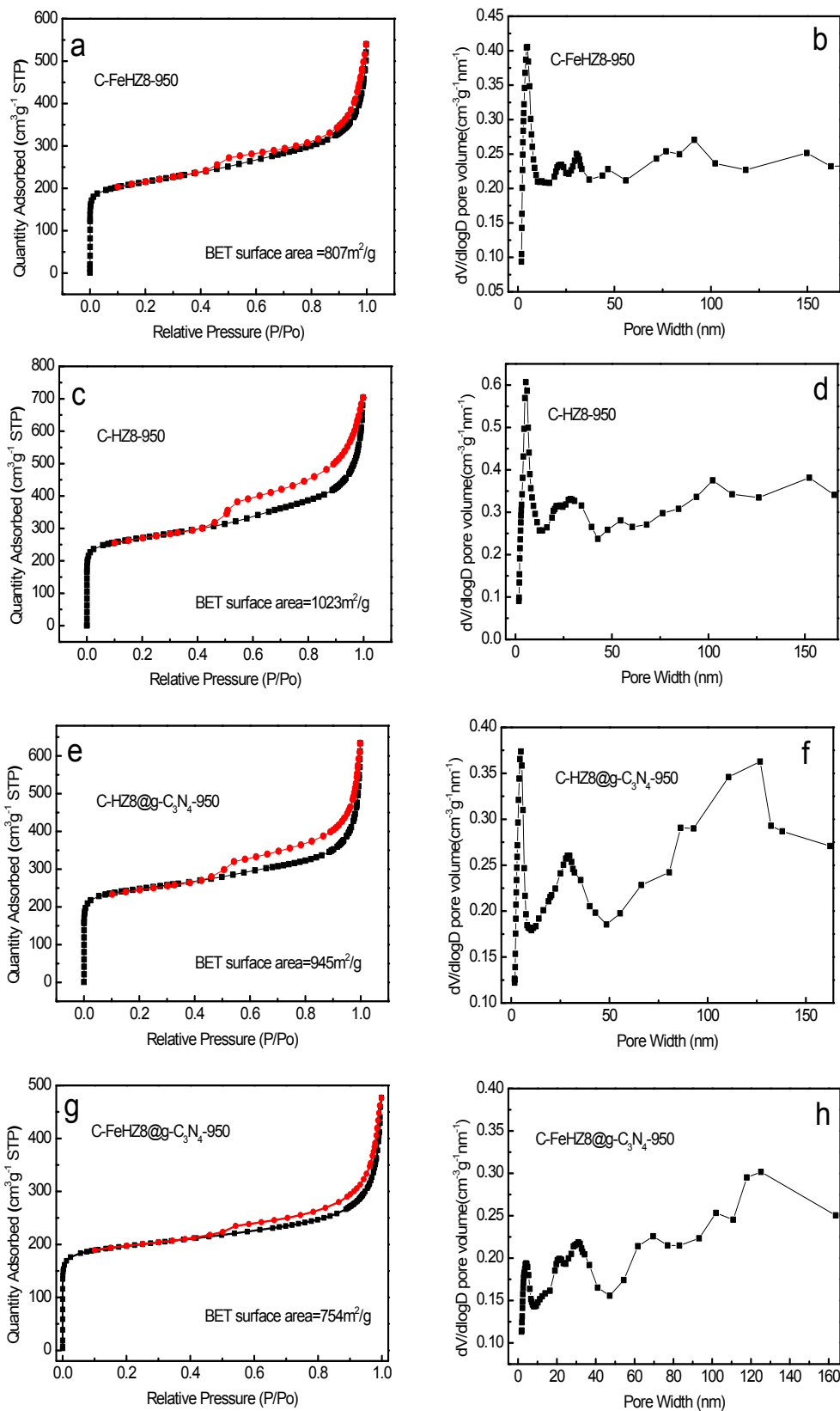


Fig. S5 N_2 adsorption/desorption isotherms and pore-size distribution curves of all sample

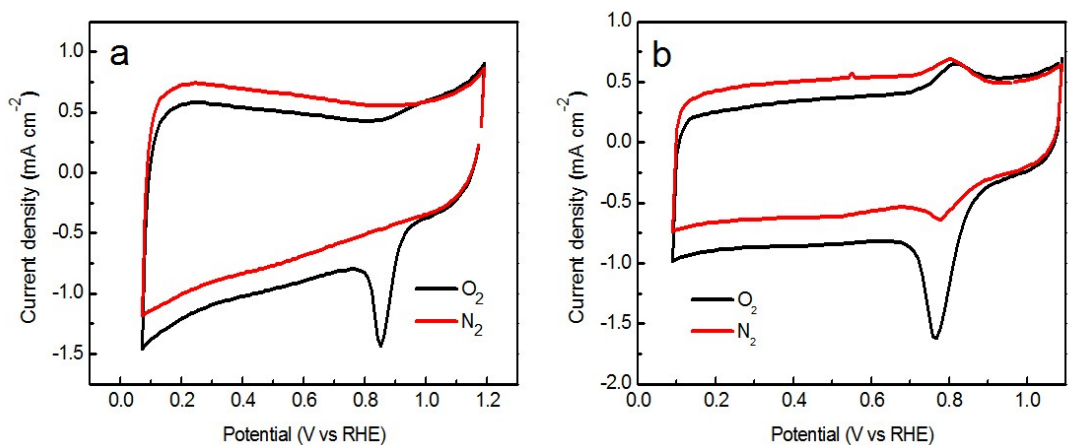


Fig. S6 CVs of C-FeHZ8@g-C₃N₄-950 in 0.1M KOH(a) and in 0.1M HClO₄ (b)

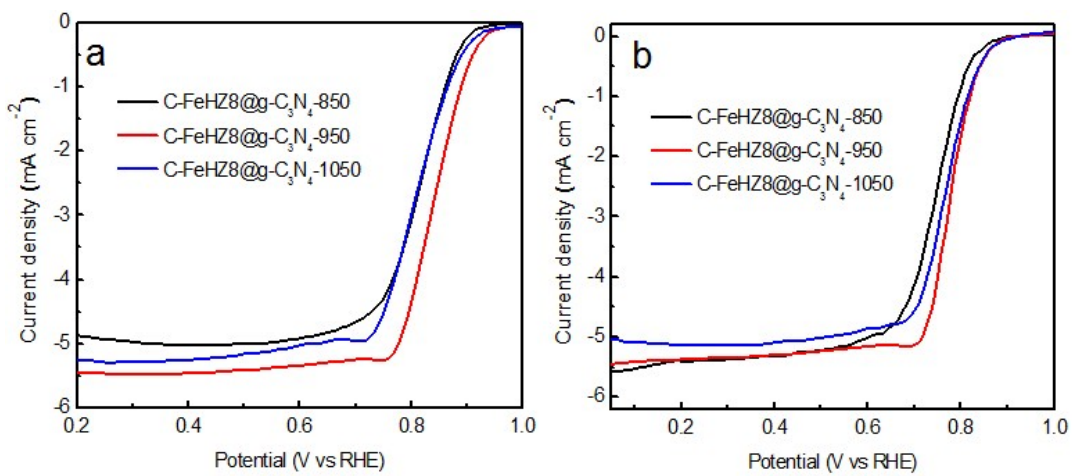


Fig. S7 LSVs of different pyrolyzed temperatures for sample in 0.1M KOH(a) and in 0.1M HClO₄ (b) (rotation rate: 1600 rpm)

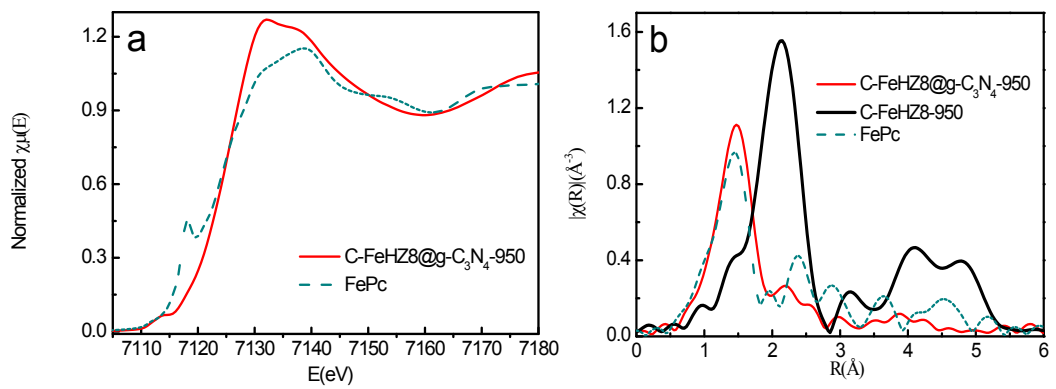
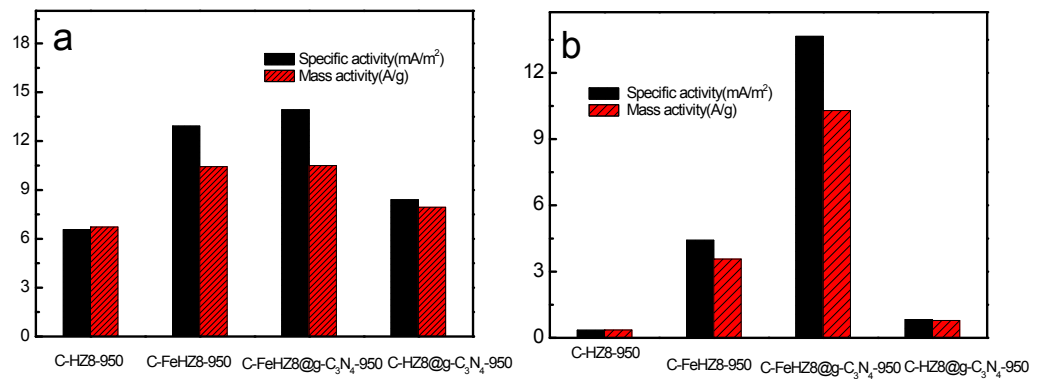


Fig. S8 *ex situ*-XANES results of iron phthalocyanine (FePc) and C-FeHZ8@g-C₃N₄-950(a); *ex situ*-Fourier-transformed EXAFS of Fe for iron phthalocyanine (FePc), C-FeHZ8-950, and C-FeHZ8@g-C₃N₄-950(b);



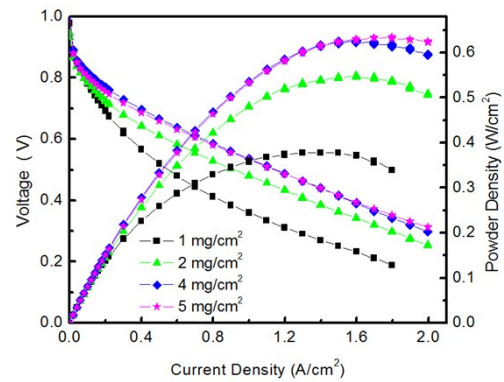


Fig. S10 Polarization curves and power-density plots for C-FeHZ8@g-C₃N₄-950 as the cathode catalyst with different loadings.

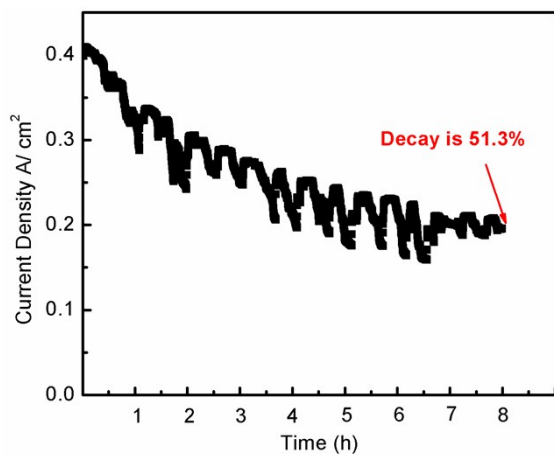


Fig. S11 Durability test of C-FeHZ8@g-C₃N₄-950 in a H₂/O₂ fuel cell

Table. S1 Comparison of the E_{onset} and $E_{1/2}$ toward ORR for non-noble metal catalysts reported and this work in alkaline medium.

Catalyst	E_{onset} vs RHE	$E_{1/2}$ vs RHE	Electrolyte	References
Co–N–GA	0.99	0.85	0.1MKOH	A1
Co-N/C	0.95	0.84	0.1MKOH	A2
Fe ₃ O ₄ /N-HCSC	1.02	0.846	0.1MKOH	A3
Co/N/C	0.94	0.83	0.1MKOH	A4
Cal-CoZIF-VXC72-H	/	0.86	0.1MKOH	A5
PPy/FeTCPP/Co	1.01	0.86	0.1MKOH	A6
Fe ₃ C@NG-800-0.2	0.98	0.83	0.1MKOH	A7
Fe/N/C	0.94	0.83	0.1MKOH	A8
Fe–N/C	1.019	0.848	0.1MKOH	A9
Fe ₃ -NG	0.965	0.826	0.1MKOH	A10
C-FeHZ8@g-C ₃ N ₄ -950	0.97	0.845	0.1MKOH	This work

A1. Fu X, Choi J Y, Zamani P, et al. Co–N decorated hierarchically porous graphene aerogel for efficient oxygen reduction reaction in acid[J]. *ACS applied materials & interfaces*, 2016, 8(10): 6488-6495. A2. Wang J, Li L, Chen X, et al. A Co-N/C hollow-sphere electrocatalyst derived from a metanilic CoAl layered double hydroxide for the oxygen reduction reaction, and its active sites in various pH media[J]. *Nano Research*, 2017, 10(7): 2508-2518. A3. Wang H, Wang W, Xu Y Y, et al. Hollow nitrogen-doped carbon spheres with Fe₃O₄ nanoparticles encapsulated as a highly active oxygen-reduction catalyst[J]. *ACS applied materials & interfaces*, 2017, 9(12): 10610-10617. A4. Li Z, Shao M, Zhou L, et al. Directed Growth of Metal–Organic Frameworks and Their Derived Carbon-Based Network for Efficient Electrocatalytic Oxygen Reduction[J]. *Advanced materials*, 2016, 28(12): 2337-2344. A5. Ni B, Ouyang C, Xu X, et al. Modifying commercial carbon with trace amounts of ZIF to prepare derivatives with superior ORR activities[J]. *Advanced Materials*, 2017, 29(27): 1701354. A6. Yang J, Wang X, Li B, et al. Novel Iron/Cobalt-Containing Polypyrrole Hydrogel-Derived Trifunctional Electrocatalyst for Self-Powered Overall Water Splitting[J]. *Advanced Functional Materials*, 2017, 27(17): 1606497. A7. Jiang H, Yao Y, Zhu Y, et al. Iron carbide nanoparticles encapsulated in mesoporous Fe–N-doped graphene-like carbon hybrids as efficient bifunctional oxygen electrocatalysts[J]. *ACS applied materials & interfaces*, 2015, 7(38): 21511-21520. A8. Ferrero G A, Preuss K, Marinovic A, et al. Fe–N-doped carbon capsules with outstanding electrochemical performance and stability for the oxygen reduction reaction in both acid and alkaline conditions[J]. *ACS nano*, 2016, 10(6): 5922-5932. A9. Zhang W, Xu X, Zhang C, et al. 3D Space-Confining Pyrolysis of Double-Network Aerogels Containing In–Fe Cyanogel and Polyaniline: A New Approach to Hierarchically Porous Carbon with Exclusive Fe–Nx Active Sites for Oxygen Reduction Catalysis[J]. *Small Methods*, 2017, 1(8): 1700167. A10. Cui X, Yang S, Yan X, et al. Pyridinic-Nitrogen-Dominated Graphene Aerogels with Fe–N–C Coordination for Highly Efficient Oxygen Reduction Reaction[J]. *Advanced Functional Materials*, 2016, 26(31): 5708-5717.

Table. S2 Comparison of the E_{onset} and $E_{1/2}$ toward ORR for non-noble metal catalysts reported and this work in acidic medium.

Catalyst	E_{onset} vs RHE		Electrolyte	References
		$E_{1/2}$ vs RHE		
PCN-FeCo/C	0.90	0.76	0.1M HClO ₄	B1
PpPD-Fe-C	0.826	0.718	0.5 M H ₂ SO ₄	B2
CPANIFe-NaCl	0.91	0.74	0.1M HClO ₄	B3
Co–N–GA	0.88	0.73	0.5 M H ₂ SO ₄	B4
5% Fe-N/C	0.834	0.735	0.1M HClO ₄	B5
FeNC-20-1000	0.90	0.77	0.1M HClO ₄	B6
Ru-N/G-750	0.89	0.75	0.1M HClO ₄	B7
(Fe _{1-x} S/N, S-MGCS) _{0.2}	0.81	0.73	0.1M HClO ₄	B8
Meso-Fe–N–C/N–G	0.83	0.72	0.1M HClO ₄	B9
FeSA-N-C	/	0.776	0.1M HClO ₄	B10
C-FeHZ8@g-C ₃ N ₄ -950	0.90	0.78	0.1M HClO ₄	This work

B1. Lin Q, Bu X, Kong A, et al. Heterometal-Embedded Organic Conjugate Frameworks from Alternating Monomeric Iron and Cobalt Metalloporphyrins and Their Application in Design of Porous Carbon Catalysts[J]. *Advanced Materials*, 2015, 27(22): 3431-3436. B2. Zhu Y, Zhang B, Liu X, et al. Unravelling the structure of electrocatalytically active Fe–N complexes in carbon for the oxygen reduction reaction[J]. *Angewandte Chemie*, 2014, 126(40): 10849-10853. B3. Ding W, Li L, Xiong K, et al. Shape fixing via salt recrystallization: a morphology-controlled approach to convert nanostructured polymer to carbon nanomaterial as a highly active catalyst for oxygen reduction reaction[J]. *Journal of the American Chemical Society*, 2015, 137(16): 5414-5420. B4. Fu X, Choi J Y, Zamani P, et al. Co–N decorated hierarchically porous graphene aerogel for efficient oxygen reduction reaction in acid[J]. *ACS applied materials & interfaces*, 2016, 8(10): 6488-6495. B5. Lai Q, Zheng L, Liang Y, et al. Metal–organic-framework-derived Fe-N/C electrocatalyst with five-coordinated Fe-Nx sites for advanced oxygen reduction in acid media[J]. *ACS Catalysis*, 2017, 7(3): 1655-1663. B6. Liu T, Zhao P, Hua X, et al. An Fe–N–C hybrid electrocatalyst derived from a bimetal–organic framework for efficient oxygen reduction[J]. *Journal of Materials Chemistry A*, 2016, 4(29): 11357-11364. B7. Zhang C, Sha J, Fei H, et al. Single-atomic ruthenium catalytic sites on nitrogen-doped graphene for oxygen reduction reaction in acidic medium[J]. *ACS Nano*, 2017, 11(7): 6930-6941. B8. Xiao J, Xia Y, Hu C, et al. Raisin bread-like iron sulfides/nitrogen and sulfur dual-doped mesoporous graphitic carbon spheres: a promising electrocatalyst for the oxygen reduction reaction in alkaline and acidic media[J]. *Journal of Materials Chemistry A*, 2017, 5(22): 11114-11123. B9. Huo L, Liu B, Zhang G, et al. 2D Layered non-precious metal mesoporous electrocatalysts for enhanced oxygen reduction reaction[J]. *Journal of Materials Chemistry A*, 2017, 5(10): 4868-4878. B10. Jiao L, Wan G, Zhang R, et al. From Metal–Organic Frameworks to Single-Atom Fe Implanted N-doped Porous Carbons: Efficient Oxygen Reduction in Both Alkaline and Acidic Media[J]. *Angewandte Chemie*, 2018, 130(28): 8661-8665.

Table. S3 Comparison of H₂–O₂ fuel cell performance of materials with published M-N-C catalysts

Catalyst	T _{cell} (K)	H ₂ /O ₂ flow rate	Back pressure	Catalyst loading(mg cm ⁻²)	P _{max} (mW·cm ⁻²)	References
20Co-NC-1100	353	200/200	30 psi	4	560	S1*
PANI-FeCo-C	353	/	0.18 MPa	4	550	S2
SA-Fe/NG	353	300/400	2 bar	2	823	S3
CNT/PC	353	400/1200	1 bar	3.05	580	S4
(CM+PANI)-Fe-C	353	200/200	2 bar	4	940	S5
PFeTTPP-1000	353	300/300	1.5 bar	4.1	730	S6
C-FeHZ8@g-C₃N₄-950	353	300/300	30 psi	4	628	This work

*[S1] Wang X X, Cullen D A, Pan Y T, et al. Nitrogen-Coordinated Single Cobalt Atom Catalysts for Oxygen Reduction in Proton Exchange Membrane Fuel Cells. Advanced Materials, 2018, 30(11): 1706758. [S2] Wu, G.; More, K. L.; Johnston, C. M.; Zelenay, P. High-performance electrocatalysts for oxygen reduction derived from polyaniline, iron, and cobalt. Science 2011, 332, 443. [S3] Yang L, Cheng D, Xu H, et al.. Unveiling the high-activity origin of single-atom iron catalysts for oxygen reduction reaction. Proceedings of the National Academy of Sciences, 2018: 201800771.[S4] Sa Y J, Seo D J, Woo J, et al. A General Approach to Preferential Formation of Active Fe–Nx Sites in Fe–N/C Electrocatalysts for Efficient Oxygen Reduction Reaction. Journal of the American Chemical Society, 2016, 138(45): 15046-15056.[S5] Chung, H. T.; Cullen, D. A.; Higgins, D.; Sneed, B. T.; Holby, E. F.; More, K. L.;Zelenay, P. Direct atomic-level insight into the active sites of a high-performance PGM-free ORR catalyst. Science 2017, 357, 479-484.[S6] Yuan S, Shui J L, Grabstanowicz L, et al. A Highly Active and Support-Free Oxygen Reduction Catalyst Prepared from Ultrahigh-Surface-Area Porous Polyporphyrin. Angewandte Chemie International Edition, 2013, 52(32): 8349-8353.